

An 850 μm survey for dust around solar mass stars

Joan Najita

National Optical Astronomy Observatory, 950 North Cherry Avenue, Tucson, AZ 85719

najita@noao.edu

Jonathan P. Williams

Institute for Astronomy, 2680 Woodlawn Drive, Honolulu, HI 96822

jpw@ifh.hawaii.edu

ABSTRACT

We present the results of an 850 μm JCMT/SCUBA survey for dust around 13 nearby solar mass stars. The dust mass sensitivity ranged from 5×10^{-3} to $0.16 M_{\oplus}$. Three sources were detected in the survey, one of which (HD 107146) has been previously reported. One of the other two submillimeter sources, HD 104860, was not detected by IRAS and is surrounded by a cold, massive dust disk with a dust temperature and mass of $T_{\text{dust}} = 33 \text{ K}$ and $M_{\text{dust}} = 0.16 M_{\oplus}$. The third source, HD 8907, was detected by IRAS and ISO at $60 - 87 \mu\text{m}$, and has a dust temperature and mass of $T_{\text{dust}} = 48 \text{ K}$ and $M_{\text{dust}} = 0.036 M_{\oplus}$. We find that the deduced masses and radii of the dust disks in our sample are roughly consistent with models for the collisional evolution of planetesimal disks with embedded planets. We also searched for residual gas in two of the three systems with detected submillimeter excesses and place limits on the mass of gas residing in these systems.

When the properties measured for the detected excess sources are combined with the larger population of submillimeter excess sources from the literature, we find strong evidence that the mass in small grains declines significantly on a ~ 200 Myr timescale, approximately inversely with age. However, we also find that the characteristic dust radii of the population, obtained from the dust temperature of the excess and assuming blackbody grains, is uncorrelated with age. This is in contrast to self-stirred collisional models for debris disk evolution which predict a trend of radius increasing with age $t_{\text{age}} \propto R_d^3$. The lack of agreement suggests that processes beyond self-stirring, such as giant planet formation, play a role in the evolutionary histories of planetesimal disks.

Subject headings: circumstellar matter — planetary systems: protoplanetary disks — planetary systems: formation — submillimeter

1. Introduction

The existence of dust around stars well beyond the protostellar phase is thought to arise from the collisions of planetesimals, the building blocks of planets, and is therefore of great interest for the clues they may reveal about the processes and timescales involved in planet formation (Backman & Paresce 1993). Indeed dusty disks are thought to be one of the most readily observable signatures of extrasolar planetary systems. Abundant dust is expected to be produced early on as part of the planet formation process itself, as planetesimals collide and grow into planetary mass objects (e.g., Kenyon & Bromley 2004a, b). Further dust production is expected as residual planetesimal disks grind themselves down to the low masses inferred for the Kuiper Belt today (e.g., Farinella, David, & Stern 2000). Giant planets in the system may sculpt the resulting debris, providing an indirect signature of their presence (e.g., Liou & Zook 1999; Ozerney et al. 2000; Quillen & Thorndike 2002; Moro-Martín & Malhotra 2002). In the context of our solar system, the age range 10–100 Myr is of interest, since it overlaps the epoch of giant planet formation and includes the epoch of formation of large bodies in the outer solar system. Also during this time period, the interaction of giant planets with a residual planetesimal disk may lead to planetary orbital migration and sculpting of the planetesimal disk.

Space based far-infrared telescopes have discovered and begun to characterize the properties of dusty disks around main sequence stars (Aumann 1985, Spangler 2000) and it is one of the primary goals of the recently launched *Spitzer Space Telescope*. Ground-based sub-millimeter observations provide useful complementary information about the properties of such disks. First, the dust mass is readily measured because the emission is almost certainly optically thin at long wavelengths. Second, by anchoring the Rayleigh-Jeans side of the spectral energy distribution (SED), constraints can be placed on the temperature and size of the emitting grains. Finally, the relatively high resolution that can be attained at these wavelengths allows investigations of the morphology of the emitting dust. Dust morphologies have been used to argue for the presence of perturbing planetary companions (Holland et al. 1998, Greaves et al. 1998, Wilner et al. 2002).

In this paper we present the results of a sub-millimeter search for dust debris surrounding 13 solar mass stars that are targets of the *Spitzer* Legacy Science Project, “Formation and Evolution of Planetary Systems” (FEPS; Meyer et al. 2004). Since a goal of the FEPS project is to place our solar system in context, the parent sample covers spectral types corresponding to approximately solar mass stars spanning a range of ages from 3 Myr to 3 Gyr. The submillimeter targets were selected from the FEPS sample with an emphasis on sources that are young (ages 10 to a few 100 Myr) and nearby (≤ 50 pc) based on estimated stellar ages for the FEPS sample (Hillenbrand et al. 2005) and Hipparcos distances. We

emphasized nearby sources in order to enable the detection of faint excesses or to place meaningful upper limits on the submillimeter flux. Our sample is shown in Table 1.

2. Observations

Photometry observations were conducted using the SCUBA bolometer at the James Clerk Maxwell Telescope (JCMT) on Mauna Kea, Hawaii between February 2003 and January 2004. The survey was only carried out in stable weather conditions when the precipitable water vapor level was less than 2 mm. Zenith optical depths ranged from 0.1 to 0.2 at 850 μm and 0.3 to 0.8 at 450 μm and the integration time spent on each source was between 40 minutes to 3 hours. The resulting rms errors varied from 1 to 3 mJy beam $^{-1}$ at 850 μm and 10 to 30 mJy beam $^{-1}$ at 450 μm . The pointing was checked via observations of bright quasars near each source after each major slew and the focus was adjusted every three hours on average, more frequently at times near sunrise and sunset. Calibration was performed by observations of Uranus, Neptune, and Mars and standard sources, CRL 618, CRL 2688, IRC+10216. Based on the agreement of the measured fluxes with those predicted for these calibrators, we estimate the photometry is accurate to within 10% at 850 μm and 30% at 450 μm .

Additional CO(3–2) observations of HD 107146 and HD 104860 were made using the 345 GHz receiver and 500 MHz acousto-optical spectrometer at the Caltech Submillimeter Observatory (CSO) in March 2003. The beamsize at this frequency is 15". The weather was very dry and stable resulting in system temperature that ranged from 450 K to 550 K. Spectra were taken in chopping mode with a throw of 120" at 0.321 Hz. The passbands were very flat over the frequency interval of interest and a single order baseline was removed from individual spectra before coadding and rebinning to 1 km s $^{-1}$ channels. Pointing was checked via observations of IRC+10216 and was accurate to 2". Antenna temperatures were converted to the main beam scale using an efficiency $\eta_{\text{mb}} = 0.65$. No emission was detected in either source at an rms noise level of 5 mK (HD 107146) and 13 mK (HD 104860) per channel.

3. Results

3.1. Submillimeter Continuum

We detected 3 objects out of our sample of 13. The measured fluxes and upper limits for the entire sample are shown in Table 1. The errors and upper limits in this Table are

based on the rms noise only and do not include the calibration uncertainty discussed above. The results are also shown graphically in the spectral energy distributions (SEDs) plotted in Figures 1, 2, and 3. To construct the SEDs, we tabulated infrared fluxes from the 2MASS All-Sky Survey, the IRAS Faint Source Catalog (FSC), and additional ISO and submillimeter fluxes from the literature (Silverstone 2000; Carpenter et al. 2005; Liu et al. 2004; Habing et al. 2001). IRAS detections were color corrected based on the effective temperature of the star for 12 and 25 μm and (typically) for a 50 K disk at 60 and 100 μm (cf. HD104860, Figure 1, where 40 K was used). For those stars not in the FSC, upper limits are plotted based on the catalog completeness (0.2 Jy at 12, 25, 60 μm and 1.0 Jy at 100 μm , non-color corrected). The stellar photosphere is shown as a Kurucz model for the appropriate stellar type scaled to the 2MASS JHK fluxes.

The brightest source detected at submillimeter wavelengths, HD 107146, is a G2 star with estimated age ~ 100 Myr. It was strong enough to map and found to be marginally resolved at 450 μm . The maps and analysis of the SED were presented in Williams et al. (2004; hereafter Paper I). Briefly, the fit to the SED implied a dust temperature of 51K and a dust mass of $0.1M_{\oplus}$. Based on the measured properties of the source, we predicted that the disk would be unusually bright in scattered light. This was confirmed in recent imaging of the system with the Hubble Space Telescope (Ardila et al. 2004). The other two submillimeter detections in our survey are associated with F8 stars: HD 104860 with an estimated age of ~ 40 Myr and HD 8907 with an age ~ 200 Myr.

For these two systems, we fit the excess above the predicted photosphere using a single temperature greybody with optical depth

$$\tau_{\lambda} = 1 - \exp[-(\lambda_0/\lambda)^{\beta}]$$

which has the desired asymptotic behavior, $\tau = 1$ for $\lambda \ll \lambda_0$ and $\tau = (\lambda_0/\lambda)^{\beta}$ for $\lambda \gg \lambda_0$. The critical wavelength, λ_0 , was set to 100 μm for consistency with previous debris disk studies (Dent et al. 2000; Wyatt, Dent & Greaves 2003). Further, because the photospheric excess was significantly detected at only two wavelengths longward of 60 μm in each case, we also fixed $\beta = 1$ based on the typical SED slope for debris disks (Dent et al. 2000) and protostellar disks (Beckwith et al. 2000). The excess was then fit by varying the dust temperature, T_{dust} , and scaling. The dust mass was determined from

$$M_{\text{dust}} = \frac{F_{850} d^2}{\kappa_{850} B_{\nu}(T_{\text{dust}})}$$

where F_{850} is the SCUBA 850 μm flux, d is the distance to the source, κ_{850} is the dust mass absorption coefficient, and B_{ν} is the Planck function.

The value of $\beta \simeq 1$ for disks is less than that observed in the ISM ($\beta \simeq 2$) and can be produced by a population of large grains (e.g., Miyake & Nakagawa 1993; Pollack et al.

1994). Independent evidence for large grains in debris disks comes from the lack of spectral features at mid-infrared wavelengths indicating that the emission arises from grains $> 10 \mu\text{m}$ in size (Jura et al. 2004) and is consistent with a collisional origin for the dust (e.g., Krivov et al. 2000).

Pollack et al. (1994) show that for spherical grains at 100 K, $\beta \leq 1$ is only achieved for radii $\geq 1 \text{ cm}$. The resulting values of κ_{850} range from 0.32 to $0.62 \text{ cm}^2 \text{ g}^{-1}$. These are a factor of 3 – 5 less than the canonical value, $\kappa = 1.7 \text{ cm}^2 \text{ g}^{-1}$, that is commonly used in studies of debris disks dating back to Zuckerman & Becklin (1993). On the other hand, porous, or fractal, dust grains can have cross-sections that are more than an order of magnitude higher than spheres per unit volume (Wright 1987). Due to the uncertainty in the dust composition and structure, we also adopt $\kappa = 1.7 \text{ cm}^2 \text{ g}^{-1}$ for ease of comparison with previous results but we note that the masses may be 3 – 5 times higher than the values assumed here.

HD 104860 was undetected by IRAS at mid- to far-infrared wavelengths, but we measured emission in excess of the photosphere at both $850 \mu\text{m}$ and $450 \mu\text{m}$ indicating a cold, massive disk. The SED is shown in Figure 1 where the photospheric excess is fit by a range of $\beta = 1$ greybodies with temperatures between 19 and 42 K. The best fit has $T_{\text{dust}} = 33 \text{ K}$ and $M_{\text{dust}} = 0.16 M_{\oplus}$. Table 2 summarizes the corresponding range of dust masses and excess luminosities. The lack of an IRAS detection and the low temperature might suggest that the submillimeter flux is due to Galactic cirrus emission but the high latitude of the source, $b = 50^\circ$, makes this unlikely. The low temperature of the dust surrounding HD104860 is similar to that of three other cold disks that have been reported around companions to early type stars (Wyatt et al. 2003).

HD 8907 was detected by IRAS at both $12 \mu\text{m}$ and $60 \mu\text{m}$ and by ISO at $60 \mu\text{m}$ and $87 \mu\text{m}$ (Silverstone 2000). The $12\mu\text{m}$ flux is photospheric, whereas the longer wavelength fluxes represent a strong excess. In the submillimeter, an excess is detected at $850 \mu\text{m}$ and marginally (2σ) at $450 \mu\text{m}$. The $\beta = 1$ greybody fit to the excess above the photosphere is tightly constrained by these points with a temperature $T_{\text{dust}} = 48 \text{ K}$, and mass $M_{\text{dust}} = 0.036 M_{\oplus}$ (Figure 2).

The SEDs of the remaining ten non-detections are shown in Figure 3. Three objects, HD 17925, HD 35850, and possibly HD 166435 show mid-infrared excesses above the stellar photospheres, but lack detections longward of $100 \mu\text{m}$. The $3\text{-}\sigma$ upper limits to the $850 \mu\text{m}$ flux and inferred disk masses are presented in Table 1. The flux upper limits were converted to mass upper limits using an average temperature for debris disks around solar type stars. Since stars with luminosities $L_* < 10 L_{\odot}$ have dust temperatures within a narrow range 33 to 56 K, averaging 50 K (Wyatt et al. 2003; Sheret et al. 2003; Sylvester et al. 2001; Liu et al. 2004; Greaves et al. 2004b), we therefore adopted an average temperature of $\langle T_{\text{dust}} \rangle = 50 \text{ K}$

in estimating the mass upper limits. Note that all the upper limits are less than or equal to the most massive disk in our sample, HD 104860, and five are less than the least massive disk, HD 8907, and therefore these non-detections provide statistically useful information. The range in source distances of course enters into the mass upper limits, but the sensitivity of the observations is nevertheless adequate to show that there is a range of disk masses present around stars of similar age. For example, for HD17925 at a distance of 10 pc and an age of 100 Myr, our mass upper limit is $0.005M_{\oplus}$. In comparison, the more distant source HD 107146 (at 28.5pc) has a similar age and a mass that is 20 times larger. These results provide further evidence for intrinsic diversity in the evolution of the circumstellar dust content of solar-type stars (cf. Meyer et al. 2004).

3.2. CO (3–2)

We can convert the upper limits on the CO(3–2) integrated intensities for HD107146 and HD104860 to upper limits on the CO gas mass assuming LTE and an excitation temperature for the gas (e.g. Scoville et al. 1986). For HD107146, we assume an excitation temperature of $T_{\text{ex}} = 50$ K based on the estimated dust temperature for the system (Paper I) and a FWHM for the line of $1.3 - 2.3 \text{ km s}^{-1}$, which is appropriate for gas at $\sim 30 - 100$ AU in orbit around a $\sim 1M_{\odot}$ star at an inclination of 25° (Ardila et al. 2004). For the more conservative limit corresponding to a FWHM of 2.3 km s^{-1} , the 3σ upper limit to the mass of gaseous CO is $M_{\text{CO}} < 2 \times 10^{-6} M_{\oplus}$. For HD104860, we assume $T_{\text{ex}} = 30$ K based on the estimated dust temperature for the system (Table 2). Since the low dust temperature is consistent with dust emission from large disk radii ($\gtrsim 100$ AU), 2 km s^{-1} FWHM is a reasonable line width. With these assumptions, the 3σ upper limit to the mass of gaseous CO is $M_{\text{CO}} < 1.3 \times 10^{-5} M_{\oplus}$. These limits vary by less than 50% for excitation temperatures in the range $T_{\text{ex}} = 25 - 100$ K.

A critical issue is the conversion from CO to total gas mass. Processes that can reduce the abundance of gas phase CO include condensation on grains and photodissociation (e.g., Dent et al. 1995; Kamp & Bertoldi 2000). If the upper limit on the CO mass is to be consistent with a primordial gas-to-dust ratio of 100 (i.e., a total gas mass of $10M_{\oplus}$), these processes must be extremely efficient given the large dust mass and our upper limit on the CO mass. For example, for the dust mass of $0.10M_{\oplus}$ measured for HD107146 (Paper I; see §3.1), a gas-to-dust ratio of 100 implies a CO to total hydrogen abundance of $n_{\text{CO}}/n_{\text{H}_2} = 2 \times 10^{-8}$ (assuming a 10% fraction of Helium by number), several orders of magnitude below the interstellar value of $n_{\text{H}_2}/n_{\text{CO}} \simeq 10^4$ (e.g., van Dishoeck et al. 1993).

For the condensation of CO on grains, an important issue is the substrate onto which

CO is adsorbed. The binding energy of CO onto water ice is 1740 K, whereas the CO–CO surface binding energy is significantly lower, 960 K (Sandford & Allamandola 1988, 1990). In their study of well-known debris disks, Kamp & Bertoldi (2000) assumed CO adsorption onto a water ice substrate, in which case where the critical grain temperature for condensation turns out to be ~ 50 K. In contrast, studies of CO condensation in protoplanetary disks have typically assumed a CO substrate where the grain condensation temperature is ~ 20 K (e.g., Aikawa et al. 1996). The relevant substrate likely depends on the thermal history of the grains in the disk.

For example, if the grains are imagined to be heated and rapidly cooled, gas phase water and CO will condense together, with CO binding to water ice. In contrast, if the grains are heated and slowly cooled, water will condense first, followed by CO. In the latter case, the abundance of CO in the gas phase relative to the number of grains is sufficient to establish a CO substrate. That is, for a gas-rich disk in which the gas-to-dust mass ratio is 100, with all of the dust in grains of radius a , and $n_{\text{CO}}/n_{\text{H}} \sim 10^{-4}$, there are $\sim 10^{13}$ CO molecules per $10\mu\text{m}$ dust grain. In comparison, there are $4\pi a^2 n_s$ binding sites available on the grain, where $n_s \simeq 1.5 \times 10^{15} \text{ cm}^{-2}$ (Tielens & Allamandola 1987), or $\sim 2 \times 10^{10}$ sites per monolayer. Thus, the condensation of only a very small fraction ($< 1\%$) of the CO is needed to establish a CO substrate. In this case, because of the low CO–CO surface binding energy, the critical temperature for condensation will be lower than that estimated by Kamp & Bertoldi (2000).

For HD107146, the measured temperature of the emitting grains is high (~ 50 K), comparable to the evaporation temperature for even CO on water ice. If the emitting grains are large and therefore at the blackbody temperature, condensation of CO on grains is not significant. Such grains would be located close to the star, at ~ 30 AU. However, if the ~ 50 K grain temperature characterizes the emission from a population of small (non-blackbody) grains located farther from the star, a larger, cooler population of grains, if also present, could potentially deplete CO from the gas phase. A distance of 100 AU is a reasonable maximum distance for the emitting grains given the spatially resolved continuum emission at $450\mu\text{m}$ (Paper I). At this distance from the star, grains $\gtrsim 100\mu\text{m}$ will be at the blackbody temperature of 28 K. Significant condensation will begin to occur when the adsorption rate onto grains exceeds the evaporation rate. For condensation onto a CO substrate, evaporation will keep CO from condensing further up to a gas phase CO density of $n_{\text{CO}} < 3 \times 10^9 \text{ cm}^{-3}$. This density limit exceeds not only the density expected at the midplane of the minimum mass solar nebula, but also the much lower densities expected in the lower mass HD107146 disk. Thus, a gas-rich disk is not expected to experience significant CO condensation for grains located anywhere from the inner radius of ~ 30 AU out to ~ 100 AU.

For HD104860, the temperature of the emitting grains is lower, ~ 30 K, and the uncertainty in temperature allows the possibility of a temperature as low as 19 K (Table 2). Given

the possibility that the emission arises from a population of relatively small (non-blackbody) grains and that larger, cooler grains may be present, it is difficult to rule out the possibility of significant CO condensation in this case.

Another process that can reduce the gas phase CO abundance is photodissociation. Kamp & Bertoldi (2000) have shown that FUV irradiation by the star and the interstellar radiation field can produce significant underabundances of CO in the disks around Vega and β Pic. Using these results, they argue that the non-detection of CO in these systems may be consistent with a primordial gas-to-dust ratio in these systems. Other studies of debris disks surrounding both A-type and solar-type stars have previously argued that CO has been significantly dissociated and that the upper limits on CO mass are consistent with primordial gas-to-dust ratios (Dent et al. 1995; Greaves et al. 2000). A later spectral-type star such as HD107146 is believed to be a negligible source of dissociating flux compared to the interstellar radiation field (Kamp & Bertoldi 2000; Greaves et al. 2000).

Following Dent et al. (1995) and Greaves et al. (2000), we can use the photodissociation models of van Dishoeck & Black (1988) to estimate the extent to which CO will be dissociated in the HD107146 disk. These models show that the relative abundance of CO is a function of both the density within and the column density through the medium. For a gas-to-dust ratio of 100, the expected disk gas mass is $10M_{\oplus}$. This corresponds to a vertical hydrogen column density of $\sim 4 \times 10^{21} - 4 \times 10^{22} \text{ cm}^{-2}$ for gas uniformly distributed in a disk 30–100 AU in radius, and a mean density of $n_{\text{H}} \sim 10^7 - 10^9 \text{ cm}^{-3}$ assuming a thermal scale height. At such large column densities, CO molecules are expected to be well-shielded. The models of van Dishoeck & Black (1988) predict that at these column densities the ratio of the CO and hydrogen column densities is $\gtrsim 10^{-4}$, several orders of magnitude larger than the ratio of 2×10^{-8} required for a primordial gas-to-dust ratio.

Thus, our CO mass limit appears to completely rule out a primordial gas-to-dust ratio for HD107146. How low might the actual gas content be? Once the total hydrogen column density of the disk begins to drop below 10^{21} cm^{-2} , the CO molecules are exposed to a higher photodissociating flux and the CO abundance relative to hydrogen declines below the well-shielded value. For a gas-to-dust ratio of order ~ 1 , we would be in the regime where the expected hydrogen column density and hydrogen number density are $N_{\text{H}} \sim 10^{20} \text{ cm}^{-2}$ and $n_{\text{H}} \sim 10^5 - 10^7 \text{ cm}^{-3}$, respectively. Model T6C of van Dishoeck & Black (1988; $n_{\text{H}} \sim 10^4 \text{ cm}^{-3}$) provides the closest match to the expected range of density. At hydrogen column densities $N_{\text{H}} \sim 10^{20} \text{ cm}^{-2}$, the model predicts that the ratio of CO and H_2 column densities is $N_{\text{CO}}/N_{\text{H}_2} \sim 10^{-5}$ or a mass ratio of $M_{\text{CO}}/M_{\text{H}_2} \sim 10^{-4}$. Thus the model implies that our upper limit on the CO mass of $2 \times 10^{-6} M_{\oplus}$ corresponds to an upper limit on the total gas mass of $\sim 0.02 M_{\oplus}$, or a gas-to-dust ratio of < 1 , significantly below the primordial value.

One of the possible flaws in this argument is that the van Dishoeck & Black models used to interpret the results were developed to address the conditions in interstellar clouds rather than those in circumstellar disks. So, for example, they describe lower density conditions than may apply to HD107146. They also do not include the possible effects of additional processes, such as advanced grain growth and stellar X-ray and UV excess irradiation, on the chemical abundance structure of the medium. We have also assumed that the gas and dust temperatures are equal, an assumption that should be examined theoretically. An improved analysis would be possible with the recent models of Gorti & Hollenbach (2004) which include such processes and more directly address the thermal and chemical structure of residual gas disks. This is a topic for future investigation.

4. Discussion

4.1. Dust Disk Radii and Masses

Single temperature greybody fits like those employed here are commonly used to interpret sparsely sampled SEDs of debris disk sources. Taken at face value, such a fit implies that the emission arises from a limited range of disk radii, in particular that the dust distribution has an inner hole. An inner hole in the dust distribution could arise in several different ways. For example, in a disk composed of icy grains, grain destruction at the water ice evaporation radius can produce an inner hole in the dust distribution. While this situation may apply to disks surrounding luminous (A- and B-type) stars that have dust temperatures ~ 100 K, similar to the water ice sublimation temperature (e.g., HR4796A—Jura et al. 1998), the low dust temperatures of the sources detected in our survey (30–50 K) suggest that this situation is not relevant here.

Primordial gas-rich disks may also develop optically thin regions as a result of grain growth and planetesimal formation. Since collisional evolution is more rapid at small radii, optically thin inner holes are expected to develop. In the gaseous outer disk, large dust masses can be maintained since gas drag can prevent grains from developing eccentric orbits and substantial relative velocities, and destructive collisions are thereby minimized. Such gas-rich outer disks with optically thin inner holes have been proposed to explain the large excesses detected in young disks systems such as TW Hya (~ 10 Myr; Calvet et al. 2002) and CoKu Tau/4 (~ 1 Myr; D’Alessio et al. 2004). Dusty disks that possess a residual gas component ($M_{\text{gas}} \lesssim 10M_{\text{dust}}$) can also develop ring-like structures as a result of gas-grain coupling in the presence of stellar radiation pressure. This situation has been proposed to explain the ring-like structures seen in systems such as HR4796A and HD141569 (e.g., Takeuchi & Artymowicz 2001).

The theoretical expectation that gaseous outer disks photoevaporate on short timescales (~ 10 Myr; Hollenbach, Yorke, & Johnstone 2000) and the lack of observations to the contrary both suggest that the above situations are unlikely to apply to our sample (age = 10–200 Myr), although they are difficult to rule out. For solar mass stars, irradiation by the central star is thought to be capable of photoevaporating away the gaseous component of the outer region ($r > 10$ AU) of a minimum mass solar nebula on a timescale of 10 Myr, if the Lyman continuum flux from the star remains at classical T Tauri levels for this length of time (Hollenbach et al. 2000). Since the Lyman continuum flux level is unlikely to continue at such levels for longer than 10 Myr, it may be difficult to dissipate more massive disks through photoevaporation by the central star alone. TW Hya may be one such example of a ~ 10 Myr old star with a substantial outer gas disk that has survived an earlier phase of energetic photoevaporation (Kastner et al. 1997; Qi et al. 2004 and references therein). Other processes such as viscous dissipation may then dominate the dissipation of the disk.

Observational support for the rapid dissipation of gaseous outer disks comes from the results of searches for gas in 1–10 Myr sources (e.g., Zuckerman, Kastner, & Forveille 1995) and known debris disk systems (e.g., Greaves et al. 2000). The limited data available for our sample (sec. 3.2) indicate an upper limit to the gas mass for HD107146 that is less than the dust mass in the system, but there is no significant constraint on the gas content of the rest of the sample. Even for HD107146, although our results apparently rule out a primordial gas-to-dust ratio for the system, the upper limit on the gas mass may still allow gas-grain coupling and radial migration of grains to play a role in sculpting the dust disk.

The possibility that these studies, which primarily do not trace H_2 directly, have underestimated the disk gas content has been raised by the surprising detection with ISO of abundant ($\sim 1M_J$) H_2 in ~ 20 Myr old debris disk systems (Thi et al. 2001). Spitzer offers an opportunity to confirm these measurements and to make similar measurements for a wider range of debris disk sources. Some uncertainty already surrounds the ISO results given since ground-based searches for mid-IR H_2 emission from younger T Tauri stars do not confirm the ISO detections (Richter et al. 2002; Sheret et al. 2003; Sako et al. 2005). In addition, recent Spitzer observations do not confirm the reported H_2 line fluxes for β Pic (C. Chen, personal communication). Whether the implied lower gas masses are representative of the general situation for debris disk systems at 20 Myr and what constraints are placed by the observations on the disk gas mass are interesting issues for the future.

Given the existing uncertainties regarding the gas dissipation timescale in disks, it is difficult to rule out the possibility that sources in our sample may have significant gaseous outer disks; gas-grain interactions may therefore contribute to the structure that is deduced from the observed SED. For the rest of the paper we assume, consistent with convention, that at the relatively advanced age of the sources in our sample (10–200 Myr) little residual

gas remains in the outer disk region. Sensitive future searches for gas in these or similar systems, such as those to be made with Spitzer as part of FEPS, may spark a reexamination of this issue.

In the absence of a substantial gaseous component to the disk, grain lifetimes are affected by both Poynting-Robertson (PR) drag and particle collisions. Collisions are expected to dominate the destruction of grains at high disk masses (e.g., Dominik & Decin 2003; Wyatt 2005). As described by Backman & Paresce (1993), the grain mutual collision time is $t_{\text{coll}} \sim P/8\sigma$ where P is the orbital period and σ is the fractional surface density (the surface filling factor) in grains. This estimate assumes that grains are on orbits that are sufficiently inclined that the grain encounters the full surface density of the disk approximately twice per orbit as it oscillates through the disk plane. The estimate also includes tangential collisions as destructive events, i.e., the collisional crosssection is 4 times the crosssectional area of individual grains. For a total dust mass M_{dust} , spread out over an area πR_{dust}^2 , internal grain density ρ_i , and average grain radius a ,

$$t_{\text{coll}} = 3000 \text{ yr } (R_{\text{dust}}/30\text{AU})^{7/2} (M_{\text{dust}}/0.1M_{\oplus})^{-1} (a/1\text{mm}).$$

Thus, for the sources in our sample with detected dust disks ($M_{\text{dust}} \sim 0.1M_{\oplus}$; Table 1), the collision timescale is significantly shorter than the age of the systems, and the observed grains must be replenished by collisions between larger bodies.

In comparison, the PR drag time for blackbody grains is

$$t_{\text{PR}} = 640 \text{ Myr } (a/1\text{mm}) (R_{\text{dust}}/30\text{AU})^2 (L_*/L_{\odot})$$

where L_* is the stellar luminosity. For the millimeter-sized grains deduced from the submillimeter observations, collisions therefore dominate as the destruction process down to dust masses $M_{\text{dust}} < 10^{-6}M_{\oplus}$, well below the dust masses inferred for the systems studied here. At dust masses above $\sim 10^{-6}M_{\oplus}$, grains are destroyed by collisions before PR drag can cause them to migrate very far from where they were created. As a result, the region of the disk that contains the collisional debris is also the region of the disk in which the colliding planetesimals that produce the debris are located.

We can estimate the orbital radii of the collisional debris for the sources detected in our sample assuming that the grains responsible for the emission are large and absorb and emit as blackbodies. The ~ 50 K dust temperature of HD107146 and HD8907 translates into grain orbital distances of approximately 30 and 48 AU respectively. The lower (~ 30 K) temperature of the dust in the HD104860 system locates the collisional debris at ~ 110 AU. We therefore infer the presence of a population of colliding planetesimals at these radii. The presence of a large planetesimal population in these young solar analogue systems at

orbital radii similar to that of the Kuiper Belt in our solar system (e.g., Jewitt & Luu 2000, PPIV) suggests their utility in understanding the early evolution of Kuiper Belt systems.

4.2. Comparison With Models

Several recent models for the collisional evolution of planetesimal disks suggest possible interpretations for these data. Dominik & Decin (2003) describe the evolution of a ring of planetesimals located at a fixed distance from the star. Assuming that the ring is in equilibrium, in the sense that grain production and destruction rates balance, the mass in small grains evolves as $M_{dust} \propto t^{-1}$ if grain destruction is dominated by mutual collisions and $M_{dust} \propto t^{-2}$ if grain destruction is governed by PR drag (see also Spangler et al. 2001). The former case would apply at early times when the disk mass is large and collisions are frequent; the latter would dominate at late times when collisions become infrequent enough the PR drag begins to dominate. The model is flexible in that it does not specify how the eccentricity and inclination distributions of the planetesimals are determined, i.e., how and when the population is stirred.

In a complementary, more prescriptive model, Kenyon & Bromley (2004) follow the evolution of a disk of planetesimals undergoing planet formation. They find that once embedded objects grow to > 1000 km in size, they stir up the surrounding planetesimals, generating a collisional cascade and accompanying debris. That is, the planetesimal disk is “self-stirred” by embedded protoplanets. Since the evolution of the disk is dominated by collisions, the growth timescale scales as the collision time $t_{coll} \propto P/\Sigma$ where P is the orbital period and Σ is the disk surface density in planetesimals. Since both the orbital speed and disk surface density decline with disk radius, the growth time is an increasing function of disk radius. Thus, a wave of planet formation propagates outward in the disk: as time progresses, the formation of embedded protoplanets excites collisions among the less massive bodies, thereby generating dust debris at successively larger characteristic radii.

In this model, the total mass in small grains in the disk remains remarkably constant with time (for perhaps as long as 1 Gyr), and subsequently decays as $\propto t^{-n}$ where $n = 1 - 2$. In contrast, the reprocessed luminosity emitted by the collisional debris begins to decline at a much earlier time (after only 1–10 Myr). This is because as the wave of planet formation moves outward, grains of a given size subtend increasingly smaller solid angles as they are located at larger distances from the star. Although the models calculated by Kenyon & Bromley are for more massive stars ($M_* = 3M_\odot$) than those in our sample, we can use the scaling of $t_{coll} \propto P/\Sigma$ to estimate the behavior that would be obtained for lower mass systems.

Comparing our results with these models, we find that the deduced size of the dust disks for the detected systems and their nominal stellar ages are roughly consistent with predictions for the evolution of dust production in collisional planetesimal disks. The Kenyon & Bromley (2004) model predicts that in a disk with a mass comparable to that of the minimum mass solar nebula that surrounds a solar mass star, it takes ~ 300 Myr for planet formation to reach 40 AU and to produce a local maximum in the dust production rate at that distance. This is comparable to the sizes (30–50 AU for HD8907 and HD107146) and ages (200 and 100 Myr respectively) of the sources studied here.

The derived dust masses for the sources detected here are $0.03 - 0.16 M_{\oplus}$. These dust masses are 2–8 times the mass in small grains that is predicted by Kenyon & Bromley (2004) to reside in a disk with the mass of the minimum mass solar nebula that is undergoing planet formation ($0.01 - 0.02 M_{\oplus}$). In the Kenyon & Bromley (2004) study, the mass in collisional debris was found to be remarkably independent of the bulk properties of the planetesimals and initial conditions other than disk mass. Instead, the dust mass was found to depend primarily on (and to be proportional to) the initial mass of solids in the disk. Interpreted in this context, the larger disk masses measured here suggest that they arise from more massive versions of the minimum mass solar nebula.

The Kenyon & Bromley (2004) calculation provides a way in which to deduce the mass of planetesimals that currently resides in the disk (see also Dominik & Decin 2003). Their results predict that at an age of 100 Myr $\sim 4 \times 10^{-4}$ of the mass in solids is in the form of grains 1 mm and smaller. Thus the measured mass in small grains implies a current mass in parent bodies of $\sim 85 M_{\oplus}$ for HD8907, $\sim 250 M_{\oplus}$ for HD107146, and $\sim 400 M_{\oplus}$ for HD104860. They also find that over the age range of the sources in our sample, the mass in small dust grains is roughly half that of the initial mass of solids in the disk. Thus the initial mass in solids in the outer planetesimal disks of the detected sources would be twice as large ($\sim 170 - 800 M_{\oplus}$). For comparison, the mass of the Kuiper Belt in our solar system today is a mere $\sim 0.1 M_{\oplus}$; in primordial times, the minimum mass solar nebula in the entire radial range 30–150 AU contained $\sim 100 M_{\oplus}$ and several $10s M_{\oplus}$ are thought to have been needed in the 30–50 AU range in order to form Pluto and QB₁-type 100m KBOs (Stern & Colwell 1997; Kenyon & Luu 1998).

Since our sample focuses on solar mass stars, it is interesting to ask what relevance these stars might have to our solar system. The large dust masses measured for the submillimeter sources detected in our study indicate initial disk planetesimal masses 2–10 times that of the minimum mass solar nebula. Such massive disks favor the production of giant planets like those in the solar system. Massive disks make it easier to form Jupiter with the possibly short lifetime of the gaseous disk (Thommes et al. 2003). So these systems may be reasonable analogues of the young solar system.

The inferred masses of the planetesimal disks in the current epoch are massive enough to play a role in determining the architectures of planetary systems. Planetesimal disks $\sim 100M_{\oplus}$ are expected to induce giant planets to migrate significantly on ~ 100 Myr timescales (Hahn & Malhotra 1999), since the clearing of a residual planetesimal disk by planets involves a significant exchange of orbital energy and angular momentum. In the case of our solar system, the interaction between a $10\text{--}100M_{\oplus}$ residual planetesimal disk and the giant planets is believed to have caused Jupiter to migrate inward and Saturn, Uranus and Neptune to migrate outward (e.g., Hahn & Malhotra 1999). In particular, the significant outward migration of Neptune (by ~ 7 AU) is thought to have sculpted the Kuiper Belt and pushed it out to the orbital distance range that it currently occupies (40–50 AU; Hahn & Malhotra 1999; Levison & Morbidelli 2003). The disks detected here appear to be sufficiently massive to induce similar migration among any giant planets that may be present.

When interpreted (literally) in the context of the Kenyon & Bromley (2004) model, the collisional debris that we have observed surrounding the ~ 100 Myr sources in our sample suggests that we are witnessing the formation of ~ 1000 km bodies at distances of 30–70 AU around nearby stars. For HD107146 and HD8907, which have debris disks at $\sim 30\text{--}50$ AU, the large bodies that are forming may correspond to proto-Plutos. These disks are comparable to the size of the Kuiper Belt in the solar system, which appears to have an edge at ~ 50 AU (Allen, Bernstein, & Malhotra 2001; Chiang & Brown 1999). The possibility of a primordial Kuiper Belt extending beyond 50 AU has been discussed in the literature (e.g., Stern 1995), and indeed HD104860 is one example of a young (40 Myr) solar-mass star with a planetesimal disk that appears to extend much beyond known extent of the Kuiper Belt in our solar system (to $R_{\text{dust}} \sim 110$ AU) and is massive enough at that distance to enable the formation of a massive perturbing object.

4.3. The properties of disks detected at $850\text{ }\mu\text{m}$

Since the inferred properties of the debris disks (planetesimal and initial disk masses) and potential implications discussed above rely on the calculations of Kenyon & Bromley (2004), one might wonder about the applicability of these models to the sources that we observed. For example, a possible limitation of the Kenyon & Bromley study is that it does not include the possible formation of giant planets at small radii and their impact on the collisional evolutionary history of an outer planetesimal disk. The presence of shepherding giant planets has often been invoked to explain the ring-like structures, observed or inferred, in disk systems over a range of ages, from ~ 1 Myr (e.g., CoKu Tau 4; D’Alessio et al. 2004) to $\gg 100$ Myr (e.g., ϵ Eri; Greaves et al. 1998). In particular the likelihood of a diversity of giant planet architectures, similar to that seen in the extrasolar planet population (Marcy

& Butler 1998), may lead to a diversity of collisional evolutionary histories that depart from those predicted by self-stirred models. One way to explore the extent of such resultant diversity and the applicability of the models to observations of outer planetesimal disks is to compare the model predictions with the collective properties of debris disks detected at submillimeter wavelengths.

We therefore collated the submillimeter excess sources from the literature and combined them with the results of our survey. In practice, almost all detections of debris disks at sub-millimeter wavelengths have been made with the SCUBA camera on the JCMT at 850 μm (Greaves et al. 2004a, 2004b; Wyatt et al. 2003, 2004; Sheret et al. 2004; Liu et al. 2004). We henceforth refer to this sample as the 850 μm disks. In the following sections we examine compare the masses, radii, and ages for the sample with the predictions of recent models for the collisional evolution of planetesimal disks.

4.3.1. *Disk Mass Evolution*

Figure 4 plots the dust masses and ages of submillimeter excess sources from the literature combined with the detections reported here. For these sources, the SCUBA fluxes were converted to masses assuming $\kappa = 1.7 \text{ cm}^2 \text{ g}^{-1}$ and dust temperatures from the literature. Non-detections are indicated in Figure 4 as $3\text{-}\sigma$ upper limits; these are calculated assuming a dust temperature of 50 K. The sources shown cover a range of spectral types, from B7 to M4. The resulting plot is similar to those that have appeared previously in the literature (e.g., Wyatt et al. 2003; Liu et al. 2004). Our detections follow the trend established by the earlier measurements, which shows a decline in the dust mass as a function of age. Such a decline is expected to result from the collisional erosion of a planetesimal disk.

Several significant selection effects complicate the interpretation of this plot. For example, the detected sources are mostly early type stars, which is likely a result of sensitivity considerations. If these more massive stars form with more massive disks, they will have preferentially larger dust masses at any given age, making them easier to detect. The higher luminosity of the central star also enhances the detectability of any surrounding dust. Another selection effect is that there are few sources ≤ 10 Myr in age that are near enough to be readily detectable at low masses. (The sources in the TW Hya and β Pic moving groups are notable exceptions.) Since such sources are typically located at larger distances than the older sources that have been detected, the lack of sources in the lower left region of the plot may simply result from sensitivity limitations. Thus, although there are no sources with low measured dust masses at 10 Myr age, there are many upper limits.

The upper right region of the plot is also not well populated, a property that seems

difficult to attribute to a selection effect. In addition, some of measurements made here (in the 10–100 Myr range) fall below the mean mass–age relation. This suggests that the detected sources represent the upper envelope of a broader distribution. This is consistent with the interpretation discussed earlier that the disks detected here arise from more massive versions of the minimum mass solar nebula. Much more massive disks are not expected since they would be gravitationally unstable.

To investigate the constraints that these data place on the evolution of debris disks, in particular the information contained in the many non-detections, we carried out a survival analysis (Feigelson & Nelson 1985) using the ASURV Rev 1.2 package (LaValley, Isobe, & Feigelson 1992). We divided the sample into a ‘young’ and ‘old’ group based on a dividing age, t_0 , and then computed the probability that they were drawn from the same population. The probabilities of similarity decreased from 7 – 12% at $t_0 = 100$ Myr to 2 – 3% at 200 Myr and down to 1 – 2%¹ at 500 Myr. Thus, there appears to be a significant difference between the ‘young’ and ‘old’ groups at a dividing age of $t_0 \sim 200$ Myr. That is, the mass in small grains decreases significantly on a ~ 200 Myr timescale.

This result is complementary to that obtained by Carpenter et al. (2004). Using survival analysis, they compared the submillimeter excess detections and upper limits obtained for a younger sample of FEPS sources with the submillimeter properties of sources in Taurus. They found no statistically significant difference between the Taurus disk population and 3–10 Myr systems, somewhat weaker evidence for a difference with the 10–30 Myr population, and a clear difference between the Taurus disk population and 30–100 Myr systems. The results presented here suggest the decline to lower dust masses continues at ages beyond ~ 200 Myr.

Although the small size (and heterogeneous nature) of the submillimeter sample makes it difficult to constrain the evolutionary behavior of the sample in greater detail, the dashed line in Figure 5 shows that the measurements can be fit by an overall $1/(\text{Age})$ dependence of dust mass vs. age with a significant spread about this trend. This overall trend is the behavior expected for a ring of planetesimals in which grain destruction is governed by collisions (Dominik & Decin 2003). This slope is also consistent with that predicted in the Kenyon & Bromley (2004) models for ages > 10 Myr. Some of the spread in the observed dust mass at a given age may be due to the range of stellar spectral types present in the sample. For example, Dominik & Decin (2003) show that a range of spectral types A0V to K3V introduces a spread of about an order of magnitude in fractional dust luminosity at

¹The precise probabilities depended on the particular statistical test used and the weighting that they give to the upper limits.

an age of 1 Gyr, a range comparable to the spread found here. Additional heterogeneity in the sample, such as a range of initial disk masses or a diversity of giant planet formation histories, would also contribute to a range in disk mass at any given age.

A caveat to these results is the possibly significant uncertainty in the estimated ages for the stars in the sample. The ages in Table 1, which derive from those estimated by FEPS, are typically uncertain by factors of 2–3. Similar errors are likely to characterize the ages of the sources from the literature. Note, however, that larger age uncertainties may characterize some sources. For example, subsequent to their selection for this study, HD88638 and HD166435 were both dropped from the FEPS sample because their Li strengths indicated ages older than the ~ 10 Myr age estimated initially for these sources. So while typical age errors of a factor of 2–3 would not significantly affect our conclusions, this issue may need to be reexamined if larger errors are eventually found to be common.

Since the survival analysis formalism used above does not account for errors in the variables, we tested the sensitivity of the inferred decline in mass with age by varying individual stellar ages by up to a factor of 3. We found that only when several systems crossed over the 200 Myr timeline did the statistics change substantially. The effect was to broaden the dividing age t_0 into an age range of 70 – 300 Myr over which an “old” population is significantly less massive than a “young” population. The two populations and the approximate border between them are shown in the two-tone greyscale in Figure 4.

4.3.2. Disk Temperatures and Inner Radii

The Kenyon & Bromley (2004) models make the simple prediction that the characteristic dust radius increases with age in a given system if self-stirring dominates the collisional evolution of planetesimal disks. We therefore compared the stellar ages with the dust radii inferred for the sample. The dust temperatures of the sources, either as measured in section 3 or from the literature, were converted to characteristic dust radii assuming blackbody grains: $R_{dust,bb} = 7.8 \times 10^4 \text{ AU } (L/L_\odot)^{0.5} T_{dust}^{-2}$. Stellar ages were taken from the literature.

Figure 5 plots the derived disk radius as a function of stellar age. No obvious correlation is found for the sample as a whole. Since the large range in stellar spectral types may obscure a trend, it would be preferable to compare the properties of a sample spanning a smaller spectral type range. Among the A stars in the sample no strong trend is found although sample statistics are admittedly poor. We might attempt to include all of the sample in a comparison by making an assumption about how the dust evolution depends on the stellar mass. If the time for debris production to reach a given radius R_d is related to the collision timescale $t_{coll} \propto P/\Sigma$ where the orbital period $P \propto R_d^{3/2} M_*^{-1/2}$ and the surface density in

planetesimals follows the slope inferred for the solar nebula $\Sigma \propto R_d^{-3/2}$, then $t_{coll} \propto R_d^3 M_*^{-1/2}$. Assuming $t_{age} \sim t_{coll}$, we would expect $t_{age} \propto R_d^3 M_*^{-1/2}$. Since the stellar mass of the sample varies by only 6 in the sample, scaling by $M_*^{1/2}$ produces only a minor variation on Figure 5. Another hypothesis might be that the initial planetesimal disk mass scales with stellar mass so that $\Sigma \propto M_* R_d^{-3/2}$. In this case $t_{coll} \sim R_d^3 M_*^{-3/2}$. The stronger dependence on M_* tightens up the distribution slightly but the spread is still large and no strong trend is apparent.

There are several caveats to these results. For one, we have assumed that the grains responsible for submillimeter excesses are large enough that they emit as blackbodies. This assumption is supported by recent results from Spitzer which show that debris disks typically do not show emission features, suggesting that the grains responsible for the excess are large $> 10\mu\text{m}$ (Jura et al. 2004). Similar spectroscopic results for the specific objects studied here would put our assumption on firmer footing.

Perhaps more significantly, sparsely sampled SEDs do not allow detailed fits that independently constrain the dust temperature and β . (The spectral slope β is a function of grain composition and shape as well as the grain size distribution.) As a result, we have typically assumed $\beta = 1$ in our fits to the dust temperatures. This may be an important source of error. For example, for HD107146, where the SED is particularly well constrained, the best fit SED implies $T = 51$ K and $\beta = 0.7$ (Williams et al. 2004), compared to a temperature of 43 K that is obtained assuming $\beta = 1$. This $\sim 20\%$ difference in temperature translates into a factor of 40% error in dust radius. This is a significant difference although much smaller than the dispersion in Figure 5.

Finally, one might ask how the inferred dust radii compare with the spatially resolved sizes of debris disks where available. The radial extent of the excess emission, when spatially resolved at long wavelengths, generally agrees within a factor of 1.5 with the dust radii estimated from the SED. Examples of such systems include Fomalhaut (Holland et al. 1998), HR4796 (Jayawardhana et al. 1998; Koerner et al. 1998), and Vega (Wilner et al. 2002). In contrast, the sizes of debris disks observed at short wavelengths (optical through near-infrared) are typically larger than the sizes inferred for the same systems based either on their SEDs at longer wavelengths or through resolved millimeter or submillimeter imaging. Examples of such systems include Vega (Su et al. 2005), β Pic (Holland et al. 1998; Kalas & Jewitt 1995) and AU Mic (Liu et al. 2004; Kalas et al. 2004). In such cases, the short wavelength scattered light probably traces a small grain population that is either being ejected or placed into eccentric orbits through a combination of radiation pressure, corpuscular (stellar wind) drag, and dynamical scattering with massive planets (e.g., Moro-Martin & Malhotra 2002, 2003b).

Thus, the available measurements suggest that the dust radii determined from the SED

assuming blackbody grains reasonably estimates the radius of the emitting grains. This could be confirmed by spatially resolving the submillimeter excess emission in a larger number of sources. When such measurements are available it will be interesting to examine the true behavior of dust radius as a function of the age of the system. At the moment, it appears that there is significant dispersion in dust radii as a function of age, with no strong correlation between these two quantities.

5. Diverse Evolutionary Histories?

In summary, the dust masses of the $850\ \mu\text{m}$ disks are roughly consistent with the predictions of recent models for the collisional evolution of planetesimal disks, in that the mass declines with time in the manner expected. However, the radii of the disks suggest a more diverse set of evolutionary histories for these systems that extend beyond histories dominated by self-stirring.

Dominik & Decin (2003) similarly recognized the need for diversity in evolutionary histories in order to explain the large dispersion in the fractional luminosities ($f_d = L_{IR}/L_*$) observed by ISO in stars spanning a range of ages. In particular, in order to explain the large fractional luminosities ($L_{IR}/L_* = 10^{-3}$) observed by ISO in Vega-like systems both young (~ 10 Myr) and old ($\gtrsim 1$ Gyr), they invoked the idea of “delayed stirring” in which a primordial planetesimal disk is allowed to collide only after a specified waiting period. They speculated that since the Kenyon and Bromley models allow for the possibility of dust production over a long timescale, as protoplanet formation progresses from small to large radii, the models may describe the underlying physical mechanism that produces luminous dust disks spanning a wide range of ages. The distribution of dust disk radii as a function of age for the $850\mu\text{m}$ disks sample suggests that this is not the whole story.

More specifically, some of the properties of individual systems are difficult to explain in detail solely with the self-stirring model. For example, HD104860 has the most massive ($0.16M_\oplus$) as well as the largest dust disk. Compared to the $\sim 40 - 50$ AU disk sizes deduced for HD107146 and HD8907, the ~ 33 K dust temperature of HD104860 corresponds to a much larger orbital distance of ~ 110 AU. While the large disk size of HD104860 may reflect the more rapid collisional evolution (and inner disk clearing) expected for more massive disks, the large size cannot be accounted for with a simple scaling of the Kenyon & Bromley results. In their model, it would take ~ 400 Myr for the wave of collisional evolution to reach 100 AU even for a system with a mass 10 times the mass of the minimum mass solar nebula, an order of magnitude larger than the published age of 40 Myr for the system.

These results suggest that processes beyond self-stirring play a significant role in the

evolutionary histories of planetesimal disks. One source of heterogeneity may be the influence of giant planets on planetesimal disks. Giant planets may clear regions of planetesimal disks and pump up the eccentricities and inclinations of planetesimals in other regions of disks, as well as sculpt the resulting dust debris. These effects have been invoked to explain the azimuthal asymmetries observed in the dust distributions surrounding some of the sources in the 850 μm disks sample (e.g., Vega; Wilner et al. 2002). It would not be surprising if giant planets were present in a large fraction of debris disk systems given the current detection statistics of precision radial velocity searches for extra-solar planets and the likelihood that more giant planets remain to be discovered at larger orbital radii (Marcy et al. 2004).

Giant planet formation is of course believed to have had a significant impact on the evolutionary history of our own Kuiper Belt. The fact that the dust content of the Kuiper Belt in the solar system is likely located far below the points in Figure 4 at $\sim 10^{-5}M_{\oplus}$ (Moro-Martin & Malhotra 2003a; Backman, Dasgupta & Stencel 1995) at an age of ~ 5 Gyr, is likely the result of a more complex evolutionary history for the Kuiper Belt than the collisional grinding of a self-stirred planetesimal disk. Indeed, the low density of Kuiper Belt objects in the solar system today and the resulting low current rate of dust production is believed to be the consequence of giant planet formation which significantly depleted the planetesimal disk in the 30–50 AU region in the early solar system (e.g., Hahn & Malhotra 1999).

Since processes such as giant planet formation may produce significant dispersion about the evolutionary trend predicted by self-stirred models, large samples of debris disk systems spanning a large range in age may be needed to recognize the expected trend of dust radius increasing with age. This may be an interesting topic to return to when larger samples are available.

6. Conclusions

To conclude, we return to the question raised at the beginning of section 4.3, on the applicability of self-stirred models to the debris disks detected in our sample. As discussed above, there is some question as to whether self-stirred models apply. The sizes and ages of the dust disks surrounding HD8907 and HD107146 appear to fit the picture described by Kenyon & Bromley (2004). If the model is applicable to these systems, it suggests that the debris in these systems arises from massive planetesimal disks with initial masses several times the minimum mass solar nebula. In contrast, the radius of the dust disk surrounding HD104860 appears too large to explain by a simple scaling of the model. More generally, the properties of the 850 μm disks sample as a whole suggest the role of additional processes,

such as giant planet formation, in contributing to the production and shaping of the debris that is observed in at least some of the systems.

On the one hand, this is encouraging for the FEPS program, since one of the aims of the program is to deduce the underlying giant planetary architectures of young solar analogues from the properties of their associated debris disks. On the other hand, the possibility that multiple processes affect the appearance of debris disks suggests that an important step toward the FEPS objective is to find ways to distinguish the relative roles of potentially multiple processes (e.g., embedded protoplanets, inner giant planets) in producing and shaping the debris. Spatially resolved observations of the debris may be one such discriminant.

Our study made use of the significant work by the FEPS team that went into compiling and characterizing the FEPS sources. We would like to thank Steve Strom and Michael Liu for careful readings of the manuscript. JPW acknowledges support from NSF grant AST-0324328. This research has made use of the SIMBAD database and the Two Micron All Sky Survey, which is a joint project of the University of Massachusetts and IPAC/Caltech, funded by NASA and NSF.

7. References

- Aikawa, Y., Miyama, S. M., Nakano, T., & Umebayashi, T. 1996, *ApJ*, 467, 684
- Allen, R. L., Bernstein, G. M., & Malhotra, R. 2001, *ApJ*, 549, L241
- Ardila, D. R., Golimowski, D. A., Krist J. E., Clampin, M., Williams, J. P., Blakeslee, J. P., Ford, H. C., Hartig G. F., & G. D. Illingworth, G. D. 2004, *ApJ*, 617, L147
- Aumann, H. H. 1985, *PASP*, 97, 885
- Backman, D. E., Dasgupta, A., & Stencel, R. E., 1995, *ApJ*, 450, L35
- Backman, D. E., & Paresce, F. 1993, in *Protostars and Planets III*, ed. Levy, E. H., & Lunine, J. I. (Tucson: University of Arizona Press), p. 1253
- Beckwith, S. V. W., Henning, T., & Nakagawa, Y. 2000, in *Protostars and Planets IV*, ed. Mannings, V., Boss, A. P., & Russell, S. S. (Tucson: University of Arizona Press), p. 533
- Calvet, N., D’Alessio, P., Hartmann, L., Wilner, D., Walsh, A., & Sitko, M. 2002, *ApJ*, 568, 1008
- Carpenter, J., Wolf, S., Schreyer, K., Launhardt, R., & Henning, T. 2005, *AJ*, 129, 1049
- Chiang, E. I., & Brown, M. E. 1999, *AJ*, 118, 1411
- D’Alessio, P., et al. 2005, *ApJ*, 621, 461
- Dent, W. R. F., Walker, H. J., Holland, W. S., & Greaves, J. S. 2000, *MNRAS*, 314, 702
- Dent, W. R. F., Greaves, J. S., Mannings, V., Coulson, I. M., & Walther, D. M. 1995, *MNRAS*, 277, L25
- Dominik, C., & Decin, G. 2003, *ApJ*, 598, 626
- Farinella, P. Davis, D. R., & Stern, S. A. 2000, in *Protostars and Planets IV*, ed. Mannings, V., Boss, A. P., & Russell, S. S. (Tucson: University of Arizona Press), p. 1255
- Feigelson, E. D. & Nelson, P. I. 1985, *ApJ*, 293, 192
- Gorti, U. & Hollenbach, D. 2004, *ApJ*, 613, 424
- Greaves, J. S. et al. 1998, *ApJ*, 506, L133
- Greaves, J. S., Coulson, I. M., & Holland, W. S. 2000, *MNRAS*, 312, L1
- Greaves, J. S., Wyatt, M. C., Holland, W. S., & Dent, W. R. F. 2004a, *MNRAS*, 351, L54
- Greaves, J. S., Holland, W. S., Jayawardhana, R., Wyatt, M. C., & Dent, W. R. F. 2004b, *MNRAS*, 348, 1097
- Habing, H. et al. 2001, *A&A*, 365, 545
- Hillenbrand, L. A., et al. 2005, submitted
- Holland, W. S. et al. 1998, *Nature*, 392, 788
- Hollenbach, D., Yorke, H. W., & Johnstone, D. 2000, in *Protostars and Planets IV*, ed. Mannings, V., Boss, A. P., & Russell, S. S. (Tucson: University of Arizona Press), p. 401
- Jayawardhana, R., Fisher, S., Hartmann, L., Telesco, C., Piña, R., & Fazio, G. 1998, *ApJ*,

503, L79

- Jura, M., Malkan, M., White, R., Telesco, C., Piña, R., & Fisher, R. S., 1998, *ApJ*, 505, 897
- Jura, M. et al. 2004, *ApJS*, 154, 453
- Kalas, P., Liu, M. C., & Matthews, B. C. 2004, *Science*, 303, 1990
- Kalas, P., & Jewitt, D. 1995, *AJ*, 110, 794
- Kamp, I. & Bertoldi, F. 2000, *A&A*, 353, 276
- Kastner, J. H., Zuckerman, B., Weintraub, D. A., & Forveille, T. 1997, *Science*, 277, 67
- Kenyon, S. J. & Bromley, B. C. 2004a, *AJ*, 127, 513
- Kenyon, S. J. & Bromley, B. C. 2004b, *ApJ*, 602, L133
- Kenyon, S. J. & Luu, J. X. 1998, *AJ*, 115, 2136
- Koerner, D. W., Ressler, M. E., Werner, M. W., & Backman, D. E. 1998, *ApJ*, 503, L83
- Krivov, A. V., Mann, I., & Krivova, N. A., 2000, *A&A*, 362, 1127
- Lavalley, M., Isobe, T., & Feigelson, E. 1992, in *ASP Conf. Ser. 25, Astronomical Data Analysis Software and Systems I*, ed. D. M. Worrall, C. Biemesderfer, & J. Barnes (San Francisco: ASP), 245
- Levison, H. F., & Morbidelli, A. 2003, *Nature*, 426, 419
- Liou, J.-C. & Zook, H. A. 1999, *AJ*, 118, 580
- Liu, M. C., Matthews, B. C., Williams, J. P., & Kalas, P. G. 2004, *ApJ*, 608, 526
- Marcy, G. W., & Butler, R. P. 1998, *ARA&A*, 36, 57
- Marcy, G. W., Butler, R. P., Fischer, D. A., & Vogt, S. S. 2004, *ASP Conf. Ser. vol. 321*, p. 3
- Meyer, M., et al. 2004, *ApJS*, 154, 422
- Miyake, K., & Nakagawa, Y. 1993, *Icarus*, 106, 20
- Moro-Martín, A. & Malhotra, R. 2002, *AJ*, 124, 2305
- Moro-Martín, A. & Malhotra, R. 2003a, *AJ*, 125, 2255
- Moro-Martín, A. & Malhotra, R. 2003b, *BAAS*, 203, 1711
- Ozernoy, L. M., Gorkavyi, N. N., Mather, J. C., & Taidakova, T. A. 2000, *ApJ*, 537, L147
- Pollack, J. B., Hollenbach, D., Beckwith, S., Simonelli, D. P., Roush, T., & Fong, W. 1994, *ApJ*, 421, 615
- Qi et al. 2004, *ApJ*, 616, L11
- Richter, M. J., Jaffe, D. T., Blake, G. A., & Lacy, J. H. 2002, *ApJ*, 572, L161
- Quillen, A. C., & Thorndike, S. 2002, *ApJ*, 578, L149
- Sako, S. et al. 2005, *ApJ*, 620, 347
- Sandford, S. A., & Allamandola, L. J. 1990, *Icarus*, 87, 188
- Sandford, S. A., & Allamandola, L. J. 1988, *Icarus*, 76, 201
- Scoville, N. Z., Sargent, A. I., Sanders, D. B., Claussen, M. J., Masson, C. R., Lo, K. Y., & Phillips, T. G. 1986, *ApJ*, 303, 416
- Sheret, I., Dent, W. R. F., Wyatt, M. C. 2004, *MNRAS*, 348, 1282

- Sheret, I., Ramsay Howat, S. K., & Dent, W. R. F. 2003, MNRAS, 343, L65
- Spangler, C., Sargent, A. I., Silverstone, M. D., Becklin, E. E., & Zuckerman, B. 2001, ApJ, 555, 932
- Silverstone, M. D. 2000, Ph. D. Thesis, UCLA
- Stern, S. A. 1995, AJ, 110, 856
- Stern, S. A. & Colwell, J. E., 1997, AJ, 114, 841
- Su, K. Y. L. et al. 2005, astro-ph/0504086
- Sylvester, R. J., Dunkin, S. K., & Barlow, M. J. 2001, MNRAS, 327, 133
- Takeuchi, T., & Artymowicz, P. 2001, ApJ, 557, 990
- Thommes, E. W., Duncan, M. J., & Levison, H. F. 2003, Icarus, 161, 431
- Tielens, A. G. G. M., & Allamandola, L. J. 1987, in "Interstellar Processes", ed. D. J. Hollenbach & H. A. Thronson, Jr. (Dordrecht: Reidel), p. 397
- Thi, W. F., et al. 2001, ApJ, 561, 1074
- van Dishoeck, E. F., & Black, J. H. 1988, ApJ, 334, 771
- Williams, J. P., Najita, J., Liu, M. C., Bottinelli, S., Carpenter, J. M., Hillenbrand, L. A., Meyer, M. R., & Soderblom, D. R. 2004, ApJ, 604, 414 (Paper I)
- Wilner, D. J., Holman, M. J., Kuchner, M. J., & Ho, P. T. P. 2002, ApJ, 569, L115
- Wright, E. L. 1987, ApJ, 320, 818
- Wyatt, M. C. 2005, A&A, 433, 1007
- Wyatt, M. C., Greaves, J. S., Dent, W. R. F., & Coulson I. M. 2005, ApJ, 620, 492
- Wyatt, M. C., Dent, W. R. F., & Greaves, J. S. 2003, MNRAS, 342, 876
- Zuckerman, B., & Becklin 1993
- Zuckerman, B., Forveille, T., & Kastner, J. H., 1995, Nature, 373, 494

TABLE 1
Summary of JCMT/SCUBA measurements

Source	SpT	Age (Myr)	d (pc)	λ (μm)	F_{ν}^{a} (mJy)	M_{d}^{b} (M_{\oplus})
1RXS J072343	K3	130	24	850	< 3.9	< 0.014
HD 17925	K1	100	10.4	850	< 7.2	< 0.005
V383 Lac	K0	60	50	850	< 8.1	< 0.12
HD 104860	F8	40	47.9	850	6.8 ± 1.2	0.16
				450	47 ± 11	
HD 8907	F8	180	34.2	850	4.8 ± 1.2	0.036
				450	22 ± 11	
HD 35850	F7	12	26.8	850	< 5.4	< 0.024
HD 984	F5	40	46.2	850	< 4.5	< 0.059
SAO 150676	F5	60	78	850	< 6.3	< 0.23
HD 88638 ^c	G5	10	37.5	850	< 4.8	< 0.041
HD 217343	G3	40	32.0	850	< 6.0	< 0.037
HD 107146	G2	100	28.5	850	20 ± 3.2	0.10
				450	130 ± 12	
HD 166435 ^c	G0	10	25.2	850	< 6.9	< 0.027
HD 77407	G0	30	30.1	850	< 5.1	< 0.028

^a Upper limits are 3σ , errors on the detections are $\pm\sigma$

^b $\kappa = 1.7 \text{ cm}^2 \text{ g}^{-1}$; $T = 50 \text{ K}$ for upper limits, 33 K for HD 104860, 48 K for HD 8907, and 51 K for HD 107146

^c May be significantly older; dropped from FEPS sample subsequent to selection for this study.

TABLE 2
 $\beta = 1$ SED fits

Source		T_{dust}	M_{dust}	L_{dust}
		(K)	(M_{\oplus})	($10^{-5} L_{\odot}$)
HD 104860	best	33	0.16	46
	min	19	0.34	8
	max	42	0.12	80
HD 8907		48	0.036	54

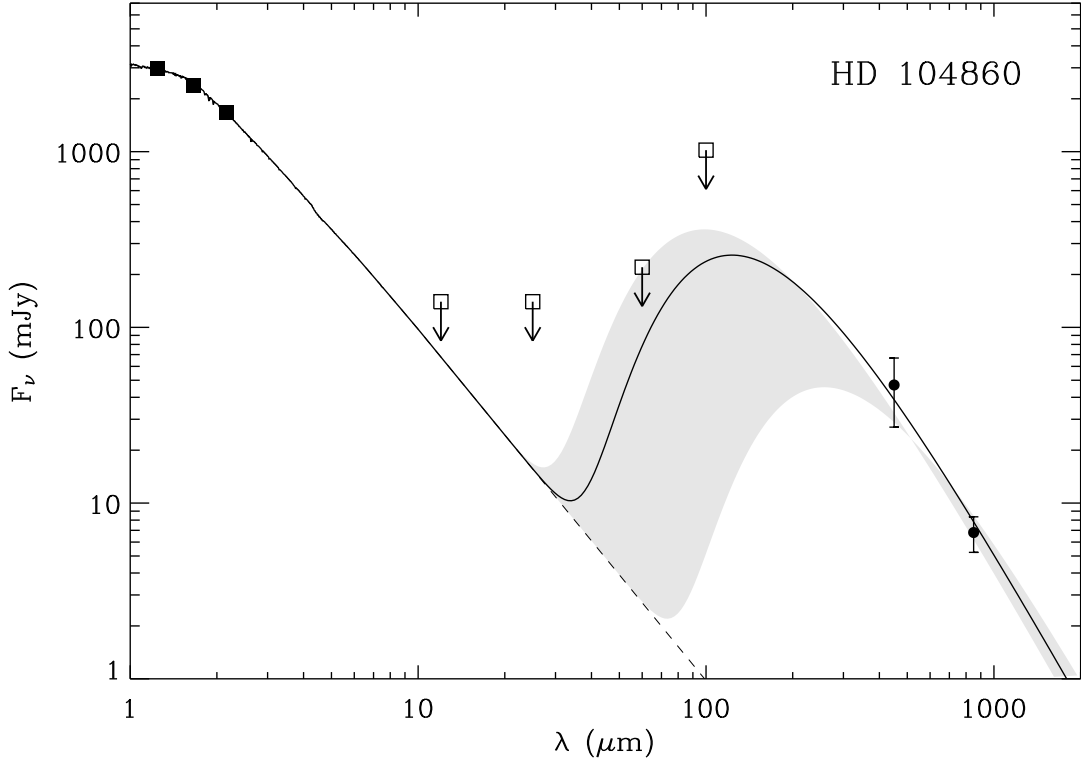


Figure 1: Spectral energy distribution of HD 104860. The three filled squares are from the 2MASS catalog. The star-disk system was not detected by IRAS; the open squares represent the FSC upper limits color-corrected for a dust temperature of 6000 K at 12 and 25 μm and 40 K at 60 and 100 μm . The filled circles show the SCUBA measurements at 450 μm and 850 μm with $\pm\sigma$ error bars. The solid line shows the best fit to the stellar photosphere and disk emission ($T_{\text{dust}} = 33$ K, $\beta = 1$), the dashed line shows the extrapolated contribution from the photosphere in the far-infrared. The grey area shows possible fits that do not violate the IRAS upper limits and lie within the systematic and calibration uncertainties of the SCUBA measurements. The corresponding range in dust mass and temperature is given in Table 2.

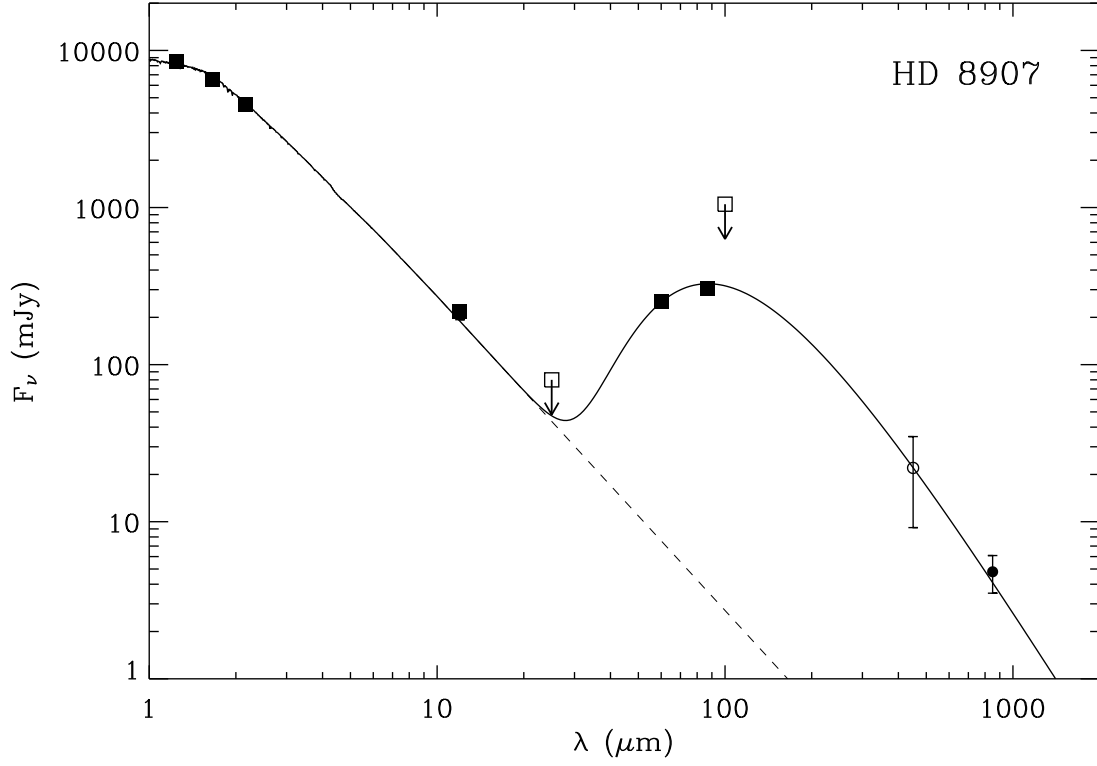


Figure 2: Spectral energy distribution of HD 8907. Detections are shown as filled symbols and include 2MASS photometry in the near-infrared, the 12 μm measurement from the IRAS FSC, 60 and 87 μm measurements from ISO, and the 850 μm SCUBA measurement. The 2 σ SCUBA detection at 450 μm is shown as an open circle. For all points the error bars are $\pm\sigma$ (when larger than the symbol size). The solid line shows the best fit to the stellar photosphere and disk emission ($T_{\text{dust}} = 48$ K, $\beta = 1$).

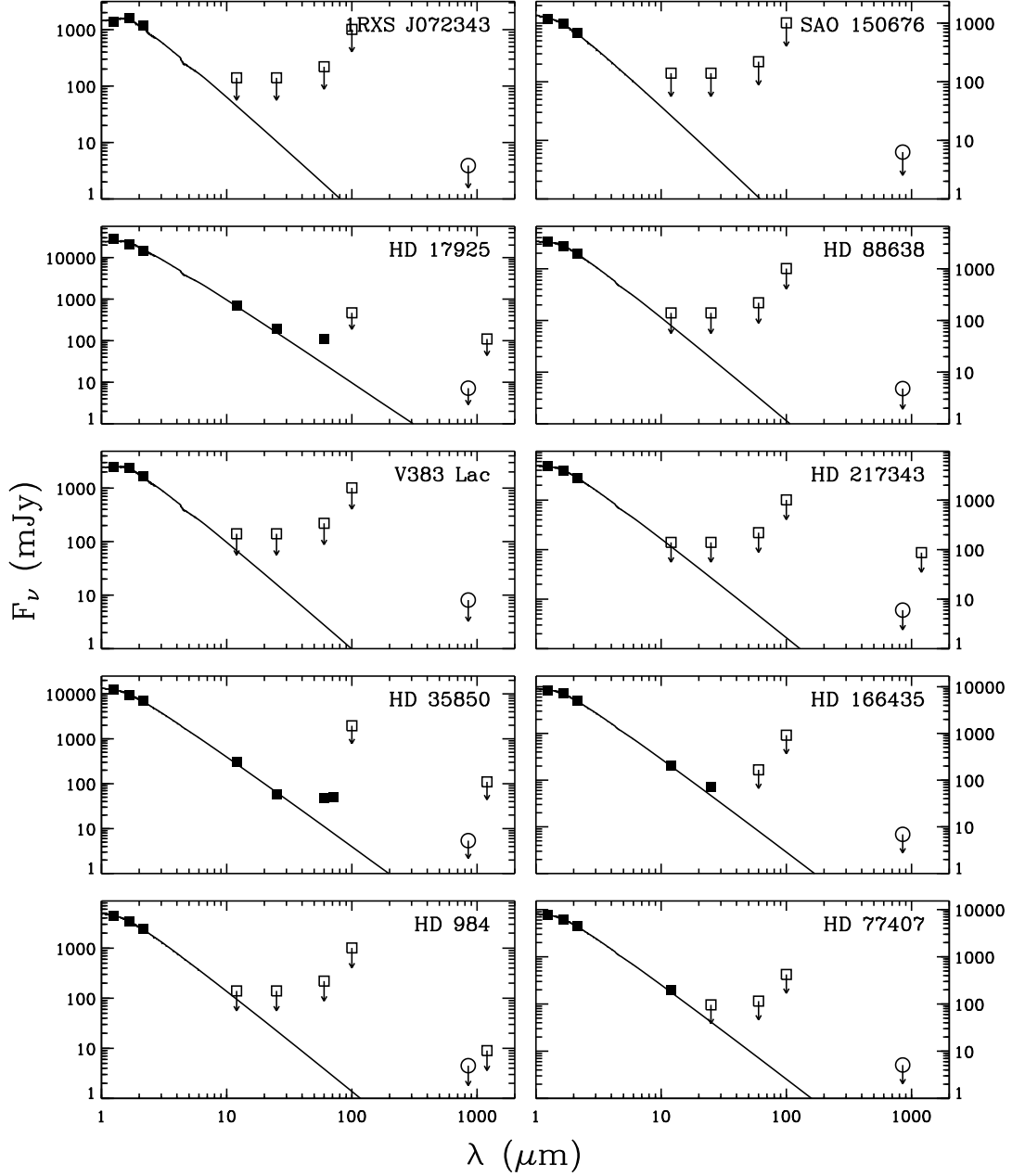


Figure 3: Spectral energy distributions for the 10 sources in the sample that were not detected in the submillimeter. The cluster of 3 points at 1 – 2 μm are fluxes from the 2MASS catalog which were used to normalize Kurucz models appropriate for each stellar type. IRAS and ISO measurements from 12–100 μm are shown as solid squares for detections and open symbols with an arrow for upper limits. A few stars were observed at 1.3 mm by Carpenter et al. (2005), and these non-detections are also shown as open squares. The 3σ SCUBA 850 μm upper limits from this work are shown as open circles.

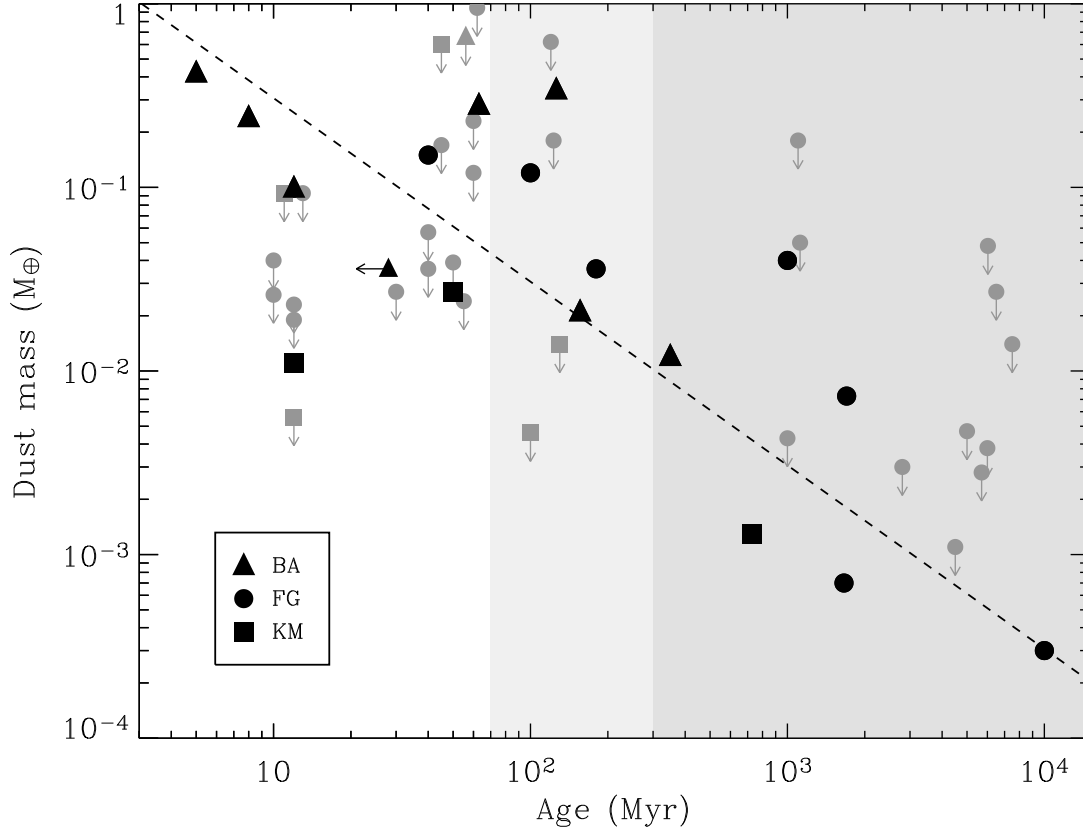


Figure 4: Disk masses versus estimated stellar age for the sample of 13 objects discussed in this paper and for other sources in the literature. Detected sources are shown in black and grey points signify 3σ upper limits based on a 50 K disk temperature, the average temperature for disks detected around solar type stars. The different symbols represent different stellar spectral types, as shown in the insert. The dashed line shows the slope expected if dust mass declines inversely with age and the darker shaded area shows the relatively older population in contrast to a significantly younger population in the unshaded region. The 70-300 Myr border between the two, due to low number statistics and age uncertainties, is shown by the lighter shaded vertical stripe.

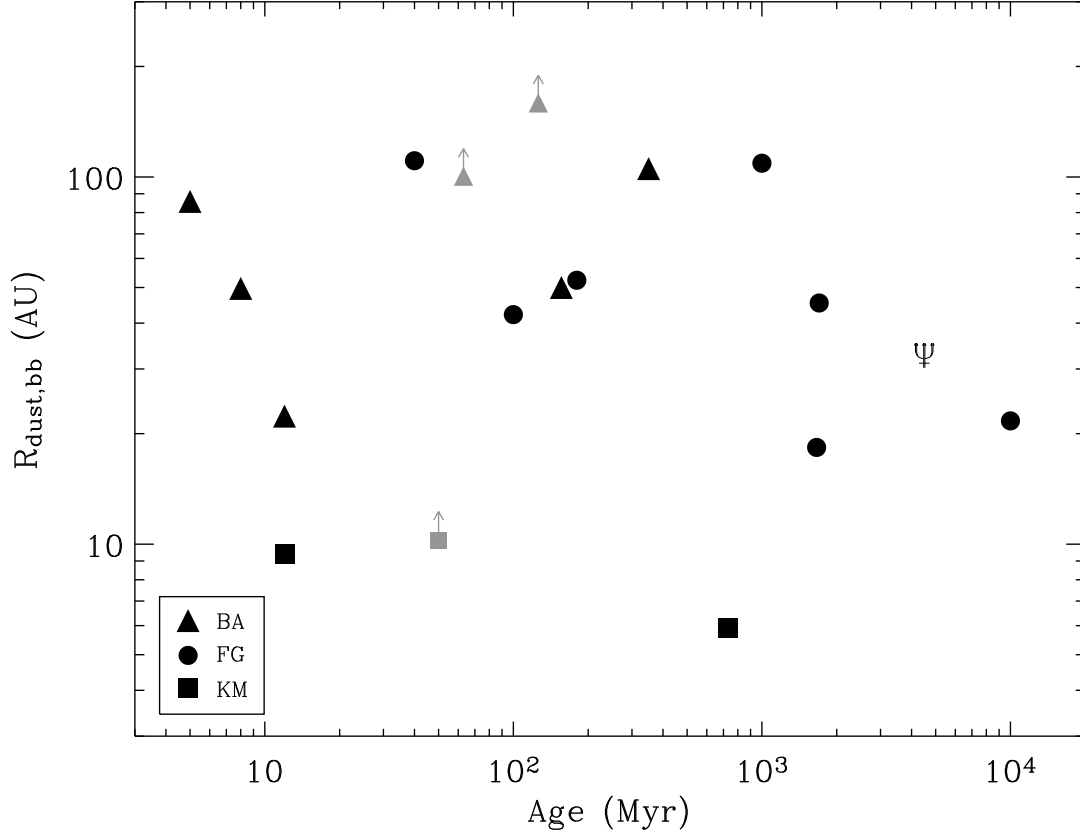


Figure 5: Characteristic dust emission radii, assuming blackbody grains, plotted against estimated stellar age for the three detections in this paper and other sub-millimeter detections in the literature. The different symbols represent different stellar spectral types, as described in Figure 4. The upper limits represent the submillimeter-only excess sources from Wyatt et al. (2003). The trident symbol indicates the orbit of Neptune in the solar system.